MICRO-RHEOLOGICAL ASSESSMENT OF NEUTROPHIL MECHANICAL PROPERTIES FOLLOWING ADHESION IN A MODEL CAPILLARY

A thesis presented to

the faculty of

the Russ College of Engineering and Technology of Ohio University

In partial fulfillment

of the requirements for the degree of

Master of Science

Anand S. Pai

August 2006

This thesis entitled

MICRO-RHEOLOGICAL ASSESSMENT OF NEUTROPHIL MECHANICAL PROPERTIES FOLLOWING ADHESION IN A MODEL CAPILLARY

by

ANAND S. PAI

has been approved for

the Department of Chemical and Biomolecular Engineering

and the College of Engineering and Technology by

David F. J. Tees

Assistant Professor of Physics and Astronomy

Dennis Irwin

Dean, Russ College of Engineering and Technology

Abstract

PAI, ANAND S., M.S., August 2006, Chemical Engineering

MICRO-RHEOLOGICAL ASSESSMENT OF NEUTROPHIL MECHANICAL PROPERTIES FOLLOWING ADHESION IN A MODEL CAPILLARY (62 pp.)

Director of Thesis: David F. J. Tees

The multistep paradigm (tethering, rolling and firm adhesion) for leukocyte adhesion in post-capillary venules has been shown to involve adhesion molecules. There has been considerable debate, however, on the relative importance of biochemical stimuli and mechanical deformation in neutrophil adhesion in lung capillaries, a process observed following bacterial infection in the body. In contrast to venules, where the leukocyte diameter (6-9 μm) is smaller than the diameter of the vessel, in lung capillaries the leukocyte diameter is larger than the capillary diameter (2 to 8 μm). In this study a micropipette aspiration assay developed to act as a flow chamber for the capillaries in the lung is described, wherein the effects of adhesion molecules (such as ICAM-1) over control (BSA) can be observed while different micropipette diameters are used to vary the extent of mechanical deformation. The 'micro-rheology' technique of tracking thermal (Brownian) motion of endogenous granules within the neutrophils using DIC video microscopy is used to extract the local intracellular viscoelastic (bulk) moduli. The results indicate regional differences in rheology with a significantly stiffer body region over the end caps which do not differ significantly in stiffness from each other. While the inclusion of adhesion molecules with deformation preserved the regional differences, an increase in viscoelastic moduli (stiffness) was seen. With the requirement for neutrophils to stay sequestered during inflammation, the results seem in line with available literature

on leukocyte sequestration mechanisms [1] and neutrophil-endothelial cell adhesion effects [2]. The effort provides an insight into the regional rheological effects of deformation and adhesion molecules on neutrophils.

Approved:

David F. J. Tees

Assistant Professor

Acknowledgments

We would like to sincerely thank Dr. Douglas Goetz and Dr. Horacio Castillo for their continued discussions during this work.

This work is supported by an award from the American Heart Association, the National Science Foundation grant BES-0547165 (DFJT) and the National Institutes of Health grant GM-057640 (DJG).

Table of Contents

List of Tables

Table **Page**

List of Figures

Figure **Page**

Chapter One: Research Background and Significance

White blood cells (leukocytes) are responsible for protecting the body against infectious pathogens. They can patrol every part of the body using a combination of circulation and migration. The critical step to this 'trafficking' is cell adhesion, which in this case is the phenomenon by which leukocytes circulating with the blood arrest and then migrate through the blood vessel to the tissue where infection is to be fought. Leukocyte adhesion to post-capillary venules has been well studied and involves a series of steps mediated by biochemical attachments. One of the predominant areas for the defense action is the pulmonary microvasculature. It is seen that bacterial infection anywhere in the body leads to sequestration of the leukocytes in the lung [1]. However in the lung microvasculature, the capillary size (2 to 8 μm) is almost half size of the leukocyte itself (typically 7-9 μm in diameter) and hence the adhesion process is likely to be different from the well-understood adhesion cascade in post-capillary venules. While red blood cells are highly deformable and can rapidly change shape to enter vessels, leukocytes, which are much less deformable, require a significant amount of time to squeeze into capillaries before moving rapidly down the vessels. Hence, it has been seen that under pathological conditions such as inflammation, leukocytes can get trapped in lung capillaries [1, 3].

The exact sequence of events involved in neutrophil sequestration and recruitment in the lung capillaries is still unclear. In particular, the influence of biochemical mediators at any stage, if any, is not clear. Molecules of the selectin and integrin family are among those extensively investigated for their roles in the immune response to

inflammation in the lung capillaries. Mice deficient in all the selectins showed normal neutrophil counts in non-inflamed lungs [4] and the same results was seen in experiments with antibodies blocking these molecules [1] demonstrating their negligible effects in maintaining the "marginated" pool (i.e. the enhanced concentration of leukocyte found in the lung capillaries that accounts for the large fraction of leukocytes found there). A number of these molecules (P-selectin and CD11/CD18), however, were shown to be required for keeping the neutrophils in the lung capillaries for extended periods (i.e "sequestered") [4] , a phenomenon critical for migration to inflamed areas. There is, thus, considerable debate on the exact mechanism for arrest in lung capillaries [1, 5-7], especially the roles of the biochemical stimuli and mechanical deformation in up- or down- regulating adhesion and hence the immune response. It is this debate about the mechanism that this work aims to address.

1.1 Blood, leukocytes and neutrophils

The 5 liters of blood that an average person has, constitutes about 7% of total body weight [8]. The blood flows from the heart into arteries that branch into smaller arterioles. These arterioles lead into capillaries where oxygen exchange takes place and the blood then returns to the heart first through small venules that join into veins. Blood is composed of about 54% liquid plasma, 45% erythrocytes (red blood cells or RBCs) and 1% leukocytes (white blood cells or WBCs) and platelets [8]. The leukocytes are further subdivided into granulocytes (that contain large granules in the cytoplasm), lymphocytes (consisting of B cells and T cells) and monocytes. The granulocytes consist of neutrophils, eosinophils, and basophils in decreasing order of typical concentration in

human blood [8]. Table 1 shows the typical concentration of each cell type in human blood [8]. In the current study we are interested in the roles played by neutrophils (the most common type of WBCs) and any further mention of leukocytes hence implies the use of neutrophils.

Cell type	**Typical concentration in human blood in cells/liter**
Red Blood Cells	5×10^{12}
Leukocytes-Granulocytes	
Neutrophils	5×10^{9}
Eosinophils	2×10^{8}
Basophils	4×10^{7}
Leukocytes-Lymphocytes	3×10^{9}
Leukocytes-Monocytes	4×10^{8}
Platelets	3×10^{11}

Table 1: Volumetric quantities of cell types in normal human blood [8].

1.2 Inflammation and its response

Inflammation is a defense reaction caused by tissue damage or injury, characterized by redness, heat, swelling, and pain [9]. The primary objective of inflammation is to localize and eradicate the irritant and repair the surrounding tissue [8, 9]. The inflammatory response has three processes: 1) dilation of capillaries to increase blood flow; 2) microvascular structural changes and escape of plasma proteins from the bloodstream; 3) leukocyte transmigration (extravasation) through endothelium to accumulate at the site of injury [1, 8, 9]. A number of molecules have been identified as inflammatory mediators and are known to bind to the specific receptors on leukocytes

and endothelial cells and hence initiate a sequence of pathways many of which aid in the adhesion process [9, 10]. Common ones used in adhesion investigation are formyl-methionyl-leucyl-phenylalanine (fMLP), histamine and chymotrypsin. Another biomolecule that is very important for lung injury investigations is lipopolysaccharide (LPS). Lipopolysaccharide (LPS) is found in the outer membrane of Gram-negative bacteria (such as Escherichia coli) and it is a potent inducer of bacterial inflammation. Bacterial sepsis anywhere in the body generates lipopolysaccharide (LPS) which also leads to massive leukocyte sequestration in the lung [11, 12].

1.3 Biochemical mediators / Adhesion Molecules

The extracellular domain of a cell adhesion protein can bind to other molecules that might be on the surface of an adjacent cell (cell-to-cell adhesion) or part of the extracellular matrix (cell-to-ECM adhesion) [8]. These adhesion molecules can be classified into many groups of homologous proteins. The types that are particularly relevant to leukocyte adhesion in the vasculature are described below.

1.3.1 Selectin Adhesion Molecules

Three selectin adhesion molecules are known, E-Selectin, L-Selectin, and P-Selectin. L-Selectin is expressed on white blood cells, while P- and E-Selectin are found on the endothelial cells [10] that line blood vessels. The selectins mediate heterotypic interactions between or among blood cells and endothelial cells during lymphocyte homing and leukocyte adhesion [13, 14]. Each type of selectin has a single Ca^{2+} dependent, C-type lectin domain, a single epidermal growth factor-like domain, and a number of complement-binding domains [15]. Selectins bind to specific carbohydrate

groups via their lectin domains. They are most commonly associated with the initial tethering and rolling events in the venular adhesion cascade [10].

1.3.2 Integrins

Integrin adhesion molecules are involved in cell-cell and cell-matrix interactions [16, 17]. Briefly, they are heterodimeric molecules, comprising of an α and a β subunit that interact noncovalently in the cell membrane [18, 19]. The binding of all integrin adhesion molecules to their ligands is Ca^{2+} or Mg^{2+} dependent [20-22], and Ca^{2+} binding sites exist on both the α- and β- subunits [23-25].

Of the many types of β subunits we are particularly interested in the β_2 subunits which are expressed exclusively on the surface of white blood cells [8]. Integrins bind to specific members of the immunoglobulin superfamily (Ig) superfamily of cell-cell adhesion molecules (discussed next). The β_2 integrins are responsible for firm binding of leukocytes to endothelial cells and migrate out of the bloodstream into the infected site [8]. The genetic disease Leukocyte Adhesion Deficiency (LAD) occurs with the inability to synthesize β_2 subunits and people with the condition suffer from repeated bacterial infections [8].

1.3.3 Immunoglobulin Super Family Adhesion Molecules

The immunoglobulin (Ig) superfamily consists of a very large group of molecules that share a common immunoglobulin domain of 70-110 amino acids, organized into 7-9 β pleated sheets [10]. They are expressed on almost every cell type, where, among other things, they are involved in cell-cell recognition, leukocyte adhesion and trafficking (ICAM-1, ICAM-2, PECAM-1, and VCAM-1) [15]. The Intercellular cellular adhesion

molecules (ICAMs) are particularly important to us as they bind to integrins expressed on leukocytes [10] and among these ICAM-1 is the best studied.

1.4 Intercellular cellular adhesion molecule -1 (ICAM-1)

ICAM-1 (also known as CD54) is a member of Immunoglobulin Super Family (IgSF). ICAM-1 associates with receptors of the integrin family, thereby mediating cell-cell interactions and allowing for signal transduction. ICAM-1 is known to bind to the integrins LFA-1 and Mac-1 [10]. ICAM-1 was specifically chosen as the adhesion molecule for this study for a number of reasons. The literature available [1, 6] indicates that in a large majority of cases selectins were proven to not be involved in adhesion in lung capillaries. It has been indicated that under normal conditions lung capillaries express low levels of ICAM-1 and no other adhesion molecules and it is only the ICAM-1 expression that is enhanced in inflamed lung capillaries [1]. Also ICAM-1 emerges as the single most common adhesion molecules expressed by the various parts of the vascular endothelium [1, 2, 6]. ICAM-1 was hence chosen as the first molecule for study to reflect the influence of adhesion molecules in-vivo.

1.5 Cell activation

Cell activation is the cellular phenomenon most commonly associated with inflammation. For leukocytes this stage is visually characterized by shape changes (extension of pseudopodia) and directed movement as well as a large number of biochemical changes within and around the cell. Activation is followed by degranulation. In degranulation the secretory granules [26] fuse with the cell membrane and release their

contents. This stage can be identified biochemically by detecting the over expression of adhesion molecules such as CD11b/CD18 on the cell surface (membrane) or the increase in certain molecules such as Ca^{2+} ions in the medium. We will use this along with the onset of shape change to detect activation of a leukocyte. It should be noted, however, that in the current studies cells that became activated (by these criteria) were not used for assessment of rheological properties.

1.6 Cytoskeleton

The cytoskeleton is a network of protein fibers in the cell cytoplasm that gives shape to a cell, holds and moves organelles, and is involved in cell movement and shape change [8]. The cytoskeleton consists of three types of fibrils [8]: microtubules, intermediate filaments, and actin microfilaments. *Actin microfilaments* (or actin microtubules) are twisted double strands consisting of protein monomers called actin. They range from 7 nm to several cm in length and are critical to shape and movement in the cytoplasm [8]. *Intermediate filaments* are made of eight subunits in rope-like strands and are important for shape and cell-cell attachments [8]. *Microtubules* are nanometer scale tubes of spiraling, two-part subunits (the monomer is tubulin) that help in chromosome movement, organelle movement and the movement of cilia and flagella [8] among other things.

As discussed above, cell activation involves shape change and hence it can be inferred that cell activation requires polymerization and depolymerization of the cytoskeletal components. The neutrophil is capable of using these processes to change its internal structure fast to give a 10 fold increase in stiffness in a matter of seconds [27].

The contribution of the cytoskeleton to cell mechanical properties, while large, is still not completely understood.

1.7 Leukocyte-Endothelium Adhesion Cascade in the inflammatory response

The leukocyte-endothelium adhesion cascade in large blood vessels is well understood. Although the restricted geometry inside capillaries does not allow for leukocyte rolling, it is still important to take a brief look at the phenomena of adhesion in venules in order to make comparisons with the current understanding of leukocyte adhesion. A blood vessel is bounded (inside) by a monolayer of endothelial cells that expresses adhesion molecules (ligands) which interact with adhesion molecules (receptors) expressed on the blood cells. The vessels themselves are surrounded by a protein-rich extra-cellular matrix, comprising a basal lamina (basement membrane), followed by other protein-rich layers [8]. The leukocyte adhesion cascade is a sequence of adhesion and activation events that ends with extravasation of the leukocyte, whereby the cell exerts its effects on the inflamed site. In post-capillary venules, leukocyte extravasation involves a cascade with at least five steps [9, 10]: tethering, rolling, slow rolling, firm adhesion, and transmigration (Fig. 1.1). Each of these five steps appears to be necessary for effective leukocyte recruitment, and blocking any of the five can severely reduce leukocyte accumulation in the tissue.

The steps in the cascade are known to be mediated by a combination of adhesion molecules. Among the best understood is the involvement of selectins and integrins.

Selectins are involved primarily in the initial steps of tethering and rolling while Integrins are the molecules associated with firm adhesion [9, 10]. The process is regulated by the expression of these molecules on the leukocyte surface and their complimentary binding molecules on the endothelial cells.

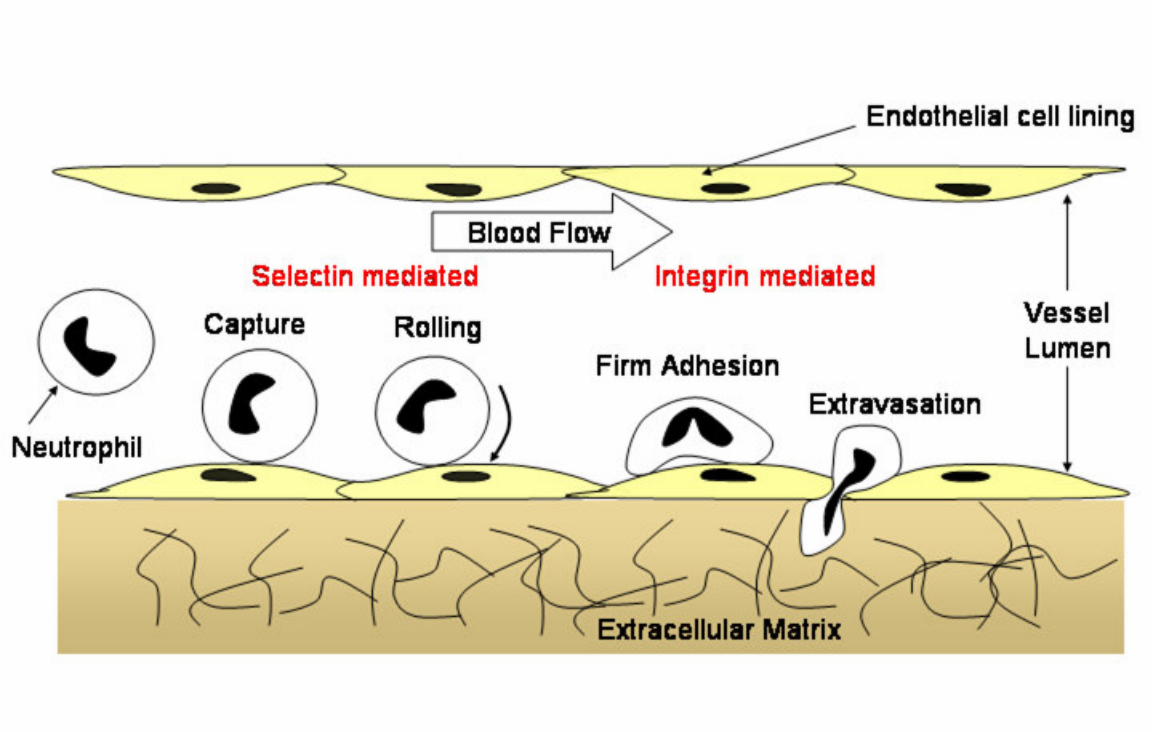

Figure 1.1. Leukocyte-endothelium adhesion cascade. The free flowing neutrophils in the blood are captured by and roll on the endothelium with the help of the selectin adhesion molecules. Integrin adhesion molecules have then been shown to be necessary for the firm adhesion and migration of the neutrophil to the site of inflammation. Adapted from [10].

1.8 Pulmonary microcirculation: Margination and sequestration in the lung

Leukocyte arrest in lung alveolar capillaries is a normal and necessary part of the response to infection or injury in the lung [28]. In the lung, much of the neutrophil sequestration and emigration occurs through the pulmonary capillaries [6]. As shown in Fig. 1.2, capillaries that surround the alveoli (where blood is exposed to oxygen) form a densely interconnected network of short segments. Lung capillaries are too narrow for the rolling adhesion mechanism seen in venules and there seems to be no initial tethering event (implying that selectins are unnecessary [1]). Mechanisms other than neutrophil–endothelial adhesion appear to mediate the initial events in neutrophil sequestration, although we have shown elsewhere that if selectins are present in the capillaries the leukocytes should arrest [29]. The current consensus supports mechanical trapping due to deformation, and retention and extravasation due to biochemical adhesion and cell activation [1, 6]. Cell activation itself, which is required for shape change, is known to be influenced by factors such as deformation and biochemical stimuli [27, 30]. Changes in deformability are most likely to result in the observed sequestration because they occur most rapidly. The deformation can act as a mechanical stimulus, and this together with biochemical mediators is hypothesized to be responsible for the neutrophil adhesion seen in the microvasculature.

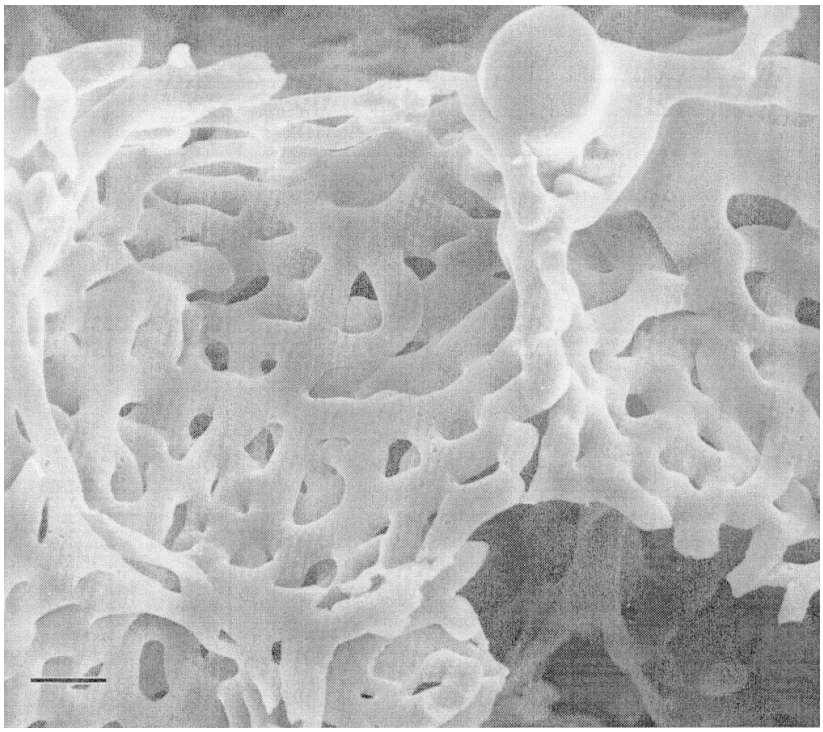

Figure 1.2. Scanning electron micrograph of a latex cast of rat lung, showing interior view of alveolar capillaries. Bar indicates 10 microns [31]. Reproduced with permission of American Physiological Society.

1.8.1 Margination

The lung capillary bed essentially consists of numerous short connected segments as shown in Fig. 1.2. Hence a blood cell must pass through about 40-100 segments while making its journey from an arteriole to venule [1]. With the capillary segments varying in size from 2-15 μm this means that each neutrophil (size 6-8 μm) has to squeeze itself through these segments numerous times on its journey through the lungs. The deformation increases the transit time of neutrophils to around 10-20 times that for a red blood cell. This increased transit time, compared to larger blood vessels, is primarily responsible for the presence of a marginated pool of neutrophils in the lungs at all times, measuring about 20-60 times the concentration in systemic circulation [1]. This pool is

extremely important in immediate immune response and its concentration depends on the stiffness of the neutrophils, indicating how deformable they are. It is hence critical to understand the effect played by deformation on a cells internal rheology and vice versa.

1.8.2 Sequestration

Sequestration is the inflammatory response showing an increased concentration of neutrophils within the inflamed lung capillaries in preparation for migration. Of the studies analyzing the effects of known biochemical mediators and the lung capillary structure on neutrophil sequestration [28, 32], a majority have found no influence of adhesion molecules on the initial steps of sequestration. It was, however, seen that once neutrophils stopped in the lung capillaries during inflammation the adhesion molecules were required to keep them stopped within the capillaries [1]. The exact roles played by biochemical events and mechanical deformations are hence not clearly understood [6].

1.9 In vitro assay to mimic arrest in capillary

1.9.1 Background

Intravital microscopy and electron microscopy of tissue sections have been used to study leukocyte adhesion in the capillary network of the lungs [3, 7, 11, 28]. These in vivo methods, however, have done little to explain the roles of mechanical and biochemical phenomena responsible for arrest due to the lack of control. In vitro assays allow much better control over the parameters that might be important for adhesion. For many years the parallel plate flow chambers have been used to investigate leukocyte adhesion in venules. These experiments have played a critical role in unraveling the

multistep paradigm that is so entrenched nowadays. The squeezing of leukocytes into lung capillaries, however, cannot be simulated with this assay because the distance between parallel plates is usually about 20 times larger than leukocyte diameter. In addition, the micropipette aspiration technique, that can generate a wide range of lung capillary-sized micropipettes, can be used to make a flow chamber with geometry similar to that of a lung capillary.

1.9.2 Micropipette aspiration

The technique of micropipette aspiration has been in use for more than two decades and has found extensive use in the analysis of leukocyte and RBC properties [33, 34]. The earliest work used the technique to measure the physical properties of bilayer membranes vesicles by simple aspiration [35] and simultaneously look at the deformation and recovery of leukocytes to better understand leukocyte rheology [33, 34]. The entrance lengths and times of the cells or bilayers under a measured pressure into the micropipettes were used to calculate the required membrane bending modulus, cortical tension and area expansion modulus. Varying the micropipette size and pressure has also proved the existence and contribution of a cortical shell structure of cytoskeleton to neutrophil rheology [34, 36]. Detailed numerical analysis [34, 37-40] of micropipette aspiration has also been done to explain the rheological movements inside cells during deformation. These studies, that have been the basis of measurement of parameters in cell rheology models, are capable of predicting the deformation of a cell in response to a suction pressure with good precision [36, 37]. This suggested that the same techniques may be used to study the dynamics of leukocyte adhesion to vascular endothelium.

1.9.3 Microrheology to probe neutrophils

Microrheology techniques have also been used to measure the rheology of soft material (including cells) non-intrusively [41, 42]. The first study by Yanai et al [43] used an optical trap to oscillate intracellular granules and use the results to calculate intracellular mechanical properties such as elasticity and viscosity. In a subsequent study Yanai et al [44] extended the work to regional rheological differences in locomoting neutrophils. It is essential to note that these studies were performed on flat surfaces and no attempt was made to mechanically deform the cells. More recently, Yap and Kamm [27] extended this analysis further by subjecting the neutrophils to deformation while observing their internal rheological properties. The study differed from the earlier studies in that it used the tracking of Brownian motion of intercellular granules to sample local rheology while deforming the neutrophils into narrow microchannels.

The previous studies that used microrheology to study regional differences in cell rheology [43, 44] and the effect of mechanical deformation on biomechanical properties [27] formed the motivation for this study. In the study by Yap and Kamm [27] the neutrophils were deformed into microfabricated rectangular channels with effective diameters 4 μm and 3.1 μm. It should, however, be noted that both channels were small enough to cause immediate activation on aspiration. The actual range of capillary diameters in the lung is, however, much larger (2-8 μm) and in vivo the cells remain passive until activated by mechanical deformation or adhesion molecules. For this reason it was decided, in our assay, to probe the neutrophils over a smaller range of deformation ratio implying larger micropipette sizes so as to observe the cells in their passive state The assay was hence designed to mimic the conditions within and the sizes of lung

capillaries to probe both the potential activators, mechanical deformation and adhesion molecules, for their influences on neutrophil internal rheology.

In a typical micropipette aspiration in this study, a single neutrophil is aspirated into a glass micropipette with inner diameter (ID) less than the diameter of the neutrophil (Fig. 1.3 A-B). During aspiration, the cell is deformed, and slowly drawn into the micropipette, and finally forms a capsule shape (Fig. 1.3 C-D). This step forms the *mechanical deformation stimulus* experienced by a cell. The important parameter for the deformation is the '*deformation ratio', R* which is defined as the ratio of the cell diameter, $\boldsymbol{D_c}$, to the inner diameter of the coated micropipette, $\boldsymbol{D_p}$, used in aspiration.

Micropipettes were first coated with BSA to prevent non-specific adhesion and allow the effects of pure deformation to be studied. The biochemical mediators are included by coating the inside of the micropipettes with adhesion molecules (in this case ICAM-1) as expressed by the endothelial cells that line the blood vessel interior. In essence these act as the *biochemical stimuli* experienced by a cell during or prior to adhesion and the *ligand concentration* acts as a measure of the magnitude of the stimulus.

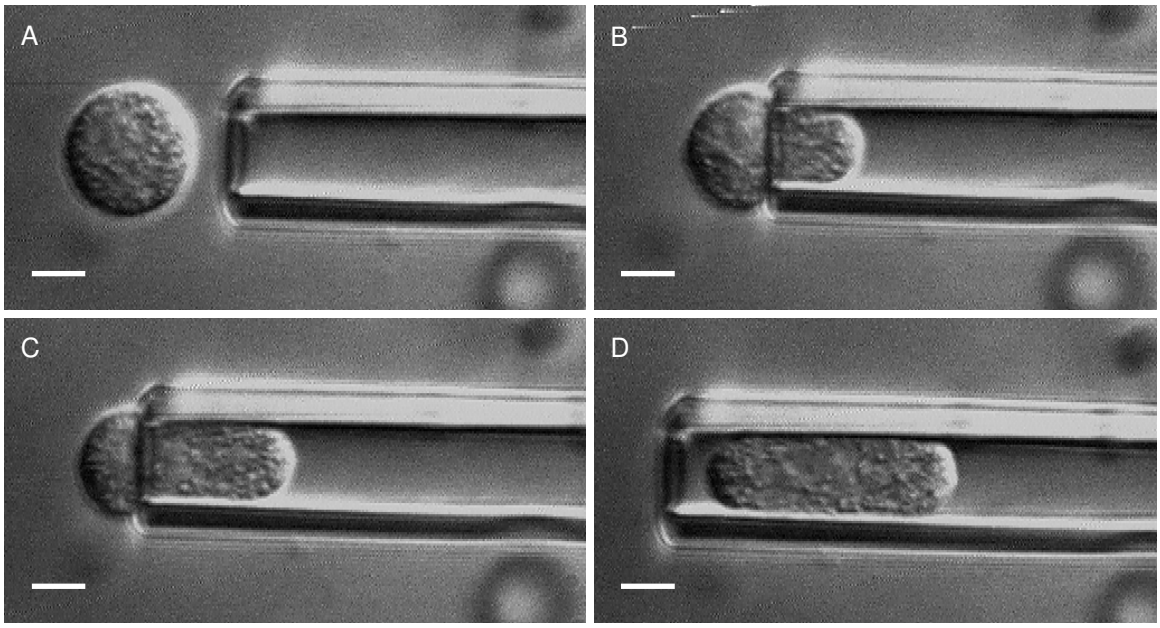

Figure 1.3. Micropipette aspiration sequence of a neutrophil (progressing in time A-D) [45]. The arrow points the direction of negative pressure and hence points to the direction of flow for the neutrophil. This particular image capture was done at 40x magnification. The white scale bar is 5 µm.

1.10 Assay: Parameters and their Control

The objective of the work was to analyze the effects of biochemical mediators and mechanical deformation on leukocyte mechanical properties during adhesion using a micropipette assay that is designed to simulate the geometry of lung capillaries. The combination of biochemical stimuli and mechanical deformation that activates a cell was observed. Previous studies [43, 44] have indicated that the biomechanical properties will differ in various regions of the interacting leukocyte so *the viscoelastic moduli in the trailing region, body region and leading region* (Fig. 1.4) were measured using particle tracking. To understand the interplay between the factors, different levels of biochemical and mechanical stimuli are used.

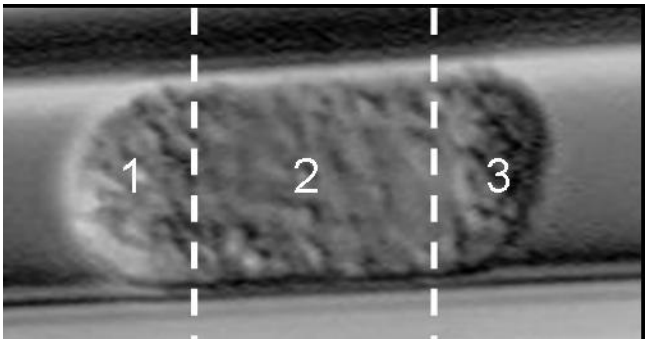

Figure 1.4. DIC microscopy image of an aspirated neutrophil with regions identified. 1)Trailing 2)Body 3)Leading

When only the effects of mechanical deformation were to be observed, Bovine Serum Albumin (BSA) was used [46]. ICAM-1 (coated using two different solution concentrations of 0.1 µg/ml and 1 µg/ml) simulated the effect of adhesion molecules present or up regulated in the lung capillaries during adhesion.

For both forms of stimulus, the aspiration procedure was the same. First (as shown in Fig. 1.3), a passive (spherical) cell, which was slightly stuck to the bottom of the chamber (so that they it doesn't move with convection) was selected for observation. The cell was then aspirated into a suitable ligand coated or control micropipette and observed for 5 minutes.

The object of this work has been to look at the passive effects of deformation [33] and hence a micropipette size range of 5 to 7.5 µm was tried. This range of sizes provided a good idea of the deformation ratios that are more likely to activate cells. This result was then used to probe the cells just beyond the stage of activation representing the range of observed pulmonary capillary sizes (2-15 µm) [1].

Chapter Two: Rheology

Rheology is defined as the flow of fluids and deformation of solids under stress and strain. For solids we should have Hooke's law where shear strain, γ is directly proportional to shear stress, σ. This *elastic behavior* can be expressed mathematically as: $\sigma = k_s \gamma$. At the other end of the spectrum we have liquids where Newton's law of viscosity posits that strain *rate* is directly proportional to shear stress. This *viscous behavior* for Newtonian fluids can be expressed using $\sigma = k_s \dot{\gamma}$. Almost all known materials and especially biological materials are 'viscoelastic' and lie in between these two regimes. We use a generalized viscosity as a function of shear rate to characterize non-Newtonian flow behavior.

2.1 Viscoelastic moduli

Viscoelastic materials are those for which the relationship between stress and strain depends on time (or frequency) of deformation. Hence to understand the nature of a viscoelastic substance the stress strain relationship should be observed under dynamic loading. The classical way to do this is to place a microscopic sample of a material in a rheometer and apply a cyclic stress to the material. The strain follows with the same frequency but with a phase lag ϕ as shown in Fig. 2.1. The stress strain relationship written in complex form is $\sigma(t) = \gamma_o \left(G'\cos(\omega t) - G''\sin(\omega t)\right)$ where G' is the elastic in-phase modulus and G'' is the viscous out of phase modulus. The stress strain relation can take into account the phase lag by writing $\sigma(t) = \gamma_o \,\mathrm{Re}\left[Ge^{i(\omega t+\phi)}\right] = \gamma_o \,\mathrm{Re}\left[Ge^{i\phi}e^{i(\omega t)}\right]$

Comparing, we see that these can be calculated as $G' = G\cos\phi$ and $G'' = G\sin\phi$. Together the complex shear modulus can be defined mathematically as $G^* = G' + iG''$ and

$$G = \left|G^*(\omega)\right| = \sqrt{\left(G'\right)^2 + \left(G''\right)^2}$$

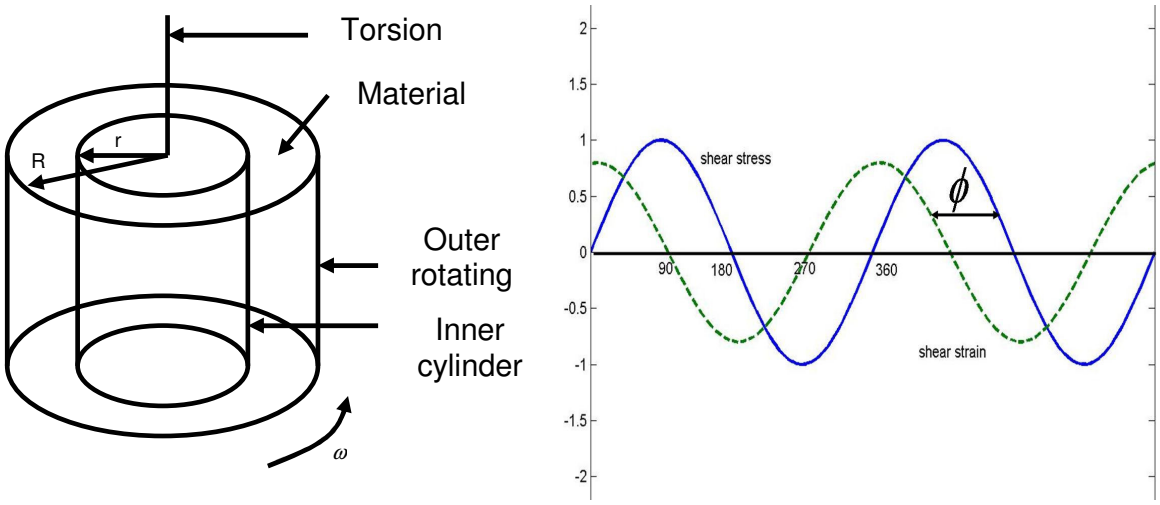

A B

Figure 2.1. Part A of the figure shows a diagrammatic view of a traditional experiment to measure viscoelasticity where the material to be measured is stressed cyclically between concentric cylinders, the outer one of which is rotating. The torsion wire (attached to inner cylinder) stretch quantifies the strain on the inner cylinder. The result is shown in graphical form in part B where ϕ is the lag between strain and stress.

2.2 Brownian motion and viscosity

The classical theory requires relatively large samples to measure the rheological properties. It is thus not possible to perform such studies on the cell cytoplasm. Micro-rheology uses the thermal motion of small particles embedded in a material in order to extract the bulk rheological properties [42]. Small tracer particles suspended in a liquid

exhibit thermal Brownian motion. The random walk that these particles perform is reduced when the particle is placed in a more viscous medium.

The parameter used to characterize the time dependent correlation random walk of a particle is its Mean Squared Displacement (MSD) defined for a two dimensional walk as:

$$\left\langle \Delta r_{2D}^2(\tau) \right\rangle = \left\langle \left\{ \left[x(t) - x(t+\tau) \right]^2 + \left[y(t) - y(t+\tau) \right]^2 \right\} \right\rangle \qquad 2.1$$

where τ is the time lag and x, y are particle positions in the 2 dimensions and the brackets indicate an average over all time. τ is the representative of the particle's time history and hence stretches from time zero to time t. The MSD in eq. 2.1 is related to simple diffusion by:

$$\left\langle \Delta r_{2D}^2(\tau) \right\rangle = 2dD\tau \qquad 2.2$$

where D is the diffusion coefficient and d the number of dimensions (of observed motion). The simplest equation for a pure viscous medium relating the diffusion D to thermal fluctuations (measured in $k_B T$ where k_B is the Boltzmann constant and T is temperature in Kelvin) is given by the Stokes-Einstein equation:

$$\frac{D}{k_B T} = \frac{1}{6\pi\eta a} \qquad 2.3$$

where η is the viscosity of the medium and a is the particle diameter. The same simplistic equation (eq. 2.3), however, cannot be used for a material that shows both elastic and viscous properties (viscoelastic materials with moduli *Gs*), a characteristic of almost all biological materials. The $\left\langle \Delta r_{2D}^2(\tau) \right\rangle$ relation for such materials can however be

elegantly related to a material's rheological properties (moduli G, G' *and* G''). (see appendix A)

The Brownian motion of the probe particles in a homogeneous elastic medium hence depends on the viscoelastic properties of the local microenvironment and measurement of a particle's mean squared displacement over time provides a value for the complex viscosity or viscoelastic moduli (G, $G´$ and $G´´$) of the medium. In the case of a neutrophil these particles are the '*granules*' present in the cytoplasm enclosed within a cell membrane. This essentially eliminates need for introduction of foreign particles into the cell for tracking and makes the procedure non-intrusive in every sense. Although particle tracking has been used to measure viscoelastic moduli in many studies of cytoskeletal properties [27, 43, 44] none of these studies have looked at the interplay between biochemical and mechanical stimuli in adhesion.

Chapter Three: Detailed Methods and Materials [47]

3.1 Purification of Neutrophils

Whole blood was obtained from human volunteers by fingerstick. Neutrophils were separated from whole blood by density gradient centrifugation using Mono-Poly Resolving Medium (M-PRM, MP Biomedicals, Aurora, Ohio) in a hematocrit tube. On centrifuging at 1000 RPM (200 g) for 15 minutes the neutrophils separated in a clear large band between plasma and Red Blood cell layer. They were extracted by cutting the tube between these bands and expelling the neutrophil layer into a solution of Hanks Balanced Salt Solution with Calcium (HBSS+) with or without 1% Bovine Serum Albumin (BSA).

3.2 Making and measurement of glass Micropipettes

Forged glass micropipettes of sizes ranging from 4-7 μm were used to study the adhesion dynamics of neutrophils. Micropipettes were formed by pulling short sections of capillary glass (0.9 mm ID) in the Micropipette/Needle Puller (Model 730, David Kopf Instruments, Tujunga, California) by the double pull technique. Micropipettes with tip internal diameter ranging from 4-7 μm were formed by changing the heat settings for the heating filament that melts the glass and the current in the solenoid that can accelerate the pull speed [47]. Once the micropipettes were made, they were forged in a microforge (MF-200; World Precision Instruments, Sarasota, Florida) to get a smooth tip. The inner diameter was measured as follows. Short sections of capillary glass (0.9 mm ID) were pulled to form fine needles using a single pull technique. These needles were sputter

coated with gold, and their images obtained with a scanning electron microscope. These images were used to develop a 5^{th} order fitting polynomials that relates the distance from the tip to the diameter of the needle tip [47]. A needle was gradually inserted into a micropipette, and the measurement of the length of the needle that enters the micropipette was used to calculate the diameter of the micropipette by substituting it into the 5^{th} order polynomial [47].

3.3 Molecules

Recombinant, soluble Human endothelium-derived ICAM-1 was the adhesion molecule used to study the dynamic adhesion of neutrophils. This was originally provided by Ray Camphausen, Wyeth Research, Cambridge, MA and was available through Dr. Douglas. J. Goetz. The solutions were further made into aliquots by series dilution into solutions of concentrations of 1 μg/ml and 0.1 μg/ml. The reason for the selection of ICAM-1 was discussed in section 1.3 on biochemical mediators.

3.4 Coating of micropipettes with Adhesion Molecules

A micropipette was first rinsed with 100% ethanol, followed by three washes with DPBS (Dulbecco's Phosphate Buffered Saline). After washing, ICAM solution at a desired concentration was pulled into the micropipette tips using a 10 ml Hamilton gastight syringe [47]. The micropipette tips were completely filled and the level held for one minute. The ICAM-1 solution was then pushed out and the micropipette tip washed three times with DPBS, followed by blocking of the entire inner surface with $DPBS^{+}$ (DPBS with Ca^{2+}/Mg^{2+}) containing 1% BSA for 1 hour at room temperature to prevent the non-specific adhesion to areas within the micropipette not coated with ICAM-1 [47].

3.5 Viewing Chamber

The design of the viewing chamber was particularly important to the experiments. The 60x oil immersion lens had a very small working distance and hence could not be used with a regular polycarbonate Petri dish on an inverted microscope because the chamber bottom was too thick. The necessary thickness was measured to be around that of a cover slip. Hence the bottom of the chamber was made with a cover-slip covering a 2 cm diameter hole drilled through the polycarbonate dish (Fig. 3.1). The hole was large enough for the lens to touch the cover slip without touching the dish so that a constant film of immersion oil could be maintained between the coverslip and the lens. The remaining part of the chamber consisted of a rectangular polycarbonate cavity open to atmosphere at the front face. The cavity was covered with a top plate made of a vinyl slide. The polycarbonate viewing chamber was filled with the cell suspension and placed gently over the microscope viewing stage.

3.6 Inverted Optical Microscope

An inverted optical microscope (Nikon Eclipse TE300) was used to make the granule displacement observations. A 60x (oil immersion; NA=1.4) lens was used in the Differential Interference Contrast (DIC) mode. DIC microscopy results in a monochromatic image wherein those regions of the specimen where the optical paths increase along a reference direction appear brighter or darker, while regions where the path differences decrease appear in reverse contrast [48]. Hence a spherical object (such as a granule) with a refractive index higher than surrounding will appear highlighted on one side with its shadow on the other side providing a much clearer view (Fig. 3.2) than phase contrast at lower magnification [48]. A video camera attached to the microscope

sent images to a video monitor (Sony Trinitron) through a Video Cassette Recorder (Sony SVO-9500MD). The image on the monitor was captured onto a PC using LabVIEW Image Acquisition Software.

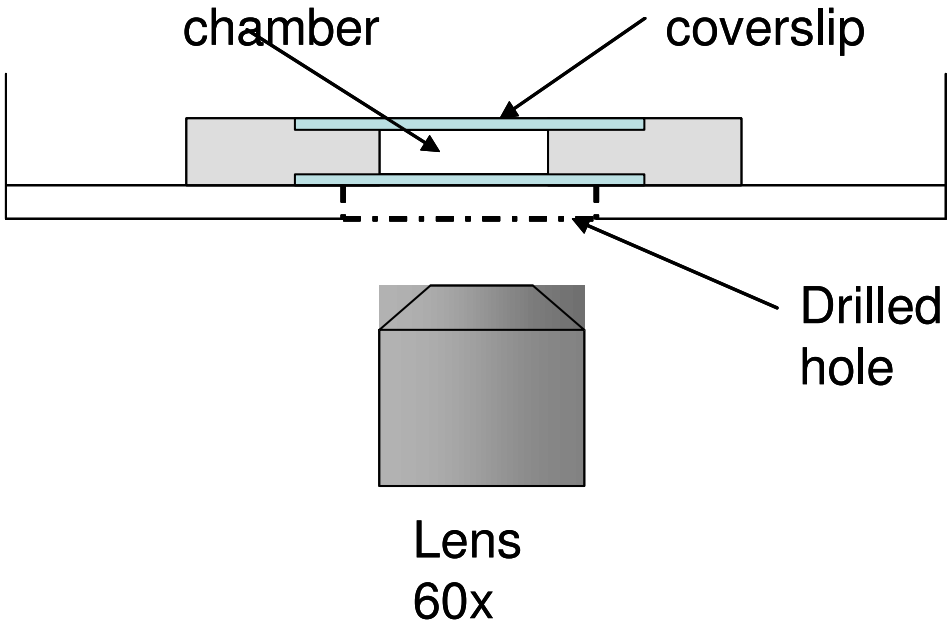

Figure 3.1. Shows a schematic of the experimental setup. The 60x lens contacts the bottom coverslip of the chamber with an oil layer in between.

3.7 Aspiration setup/procedure

The polycarbonate viewing chamber was filled with the neutrophil suspension. The chamber was placed gently over the heated stage of an inverted microscope, just above the objective lens [47]. A micropipette with or without a coating of adhesion molecules on the inner surface was attached to a manometer and mounted on a micromanipulation system. Once the micropipette was in the chamber, cells were aspirated into the micropipette using a pressure difference created with the help of the

manometer. Pressure difference from 0 to 20 mm of water can be generated precisely using a micrometer on the manometer [47].

3.8 Image processing

After an experiment, the videotapes were analyzed to extract the viscoelastic parameters for a given experimental condition. One single data point (for either modulus) was obtained by tracking an individual granule within a neutrophil (deformed or undeformed). This was done with the help of a particle tracking interface created in LabVIEW. The interface tracks a particle's mean squared displacement over a period of time to make predictions of the viscoelastic moduli of the cell interior in the neighborhood of the particle. Figure 3.2 shows a deformed cell where a particle was chosen (arrow) and tracked. The image processing interface is shown in Fig. 3.3. Briefly, an area of interest (having granules) was chosen within a cell. The interface then displayed a histogram of pixel intensities in the chosen area, as shown in the center graph of Fig. 3.3. Based on the peak of this histogram a choice of threshold intensity was made for the computer to identify particles. If the computer was unable to identify particles the threshold intensity was changed or a new area of interest chosen. If particles were identified, any one of them were selected for tracking and their displacement stored. The graph on the right in Fig. 3.3 shows the actual displacement of a selected particle in 2 dimensions.

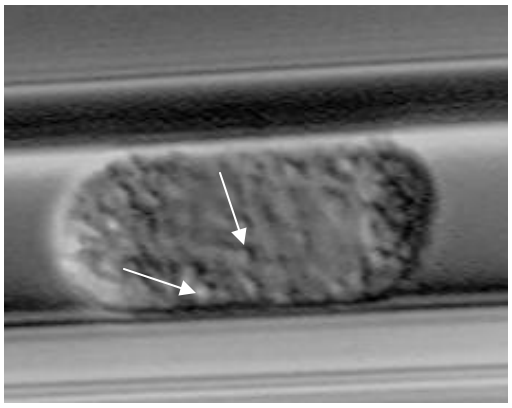

Figure 3.2. DIC microscopy image of an aspirated neutrophil. The arrows point to potential granules that can be tracked.

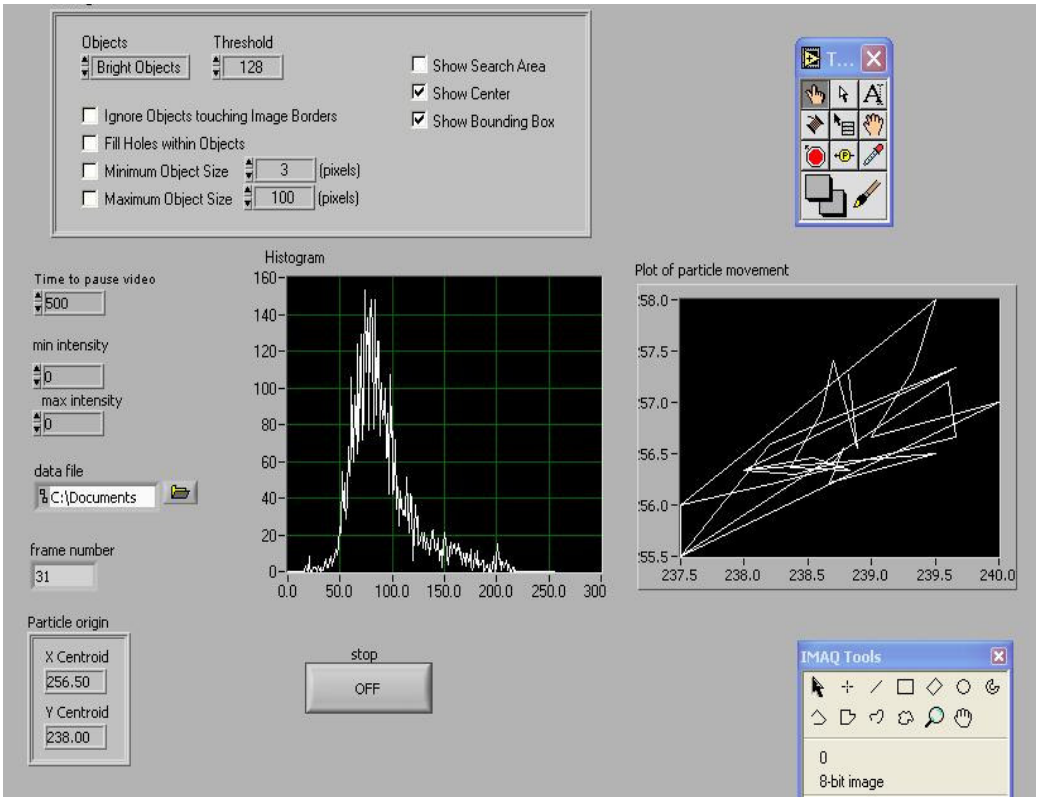

Figure 3.3. A view of the particle tracking interface in LabVIEW. The graph to the right shows the x-y displacement of the particle in two dimensions.

3.9 Extracting rheological parameters from MSD data

The particle tracking interface provides us 2D x-y displacements of the chosen granules as in Fig. 3.3. This data is converted to the Mean Squared Displacement (MSD), or Δr_{2D}^2, using the definition: $\Delta r_{2D}^2 = \left\{ [x(t) - x(0)]^2 + [y(t) - y(0)]^2 \right\}$ (3.1)

The MSD data Δr_{2D}^2 varies with time so we write $\Delta r_{2D}^2(t)$. Assuming that the cytoplasm is isotropic [41] the 2D displacement can be transformed into 3D displacement by

$$\left\langle \Delta r_{3D}^2 \right\rangle = \left(\frac{3}{2} \right) \times \left(\left\langle \Delta r_{2D}^2 \right\rangle \right) \tag{3.2}$$

For any further analysis, the 3D MSD data has to be expressed in functional form. The data is fit with a logarithmic function

$$\log\left(\left\langle \Delta r^2(t) \right\rangle \right) = a + b\log(t) + c\{\log(t)\}^2 \tag{3.3}$$

A non-linear least squares fit provides the coefficients *a,b* and *c*. It is now possible to find expected value as a function of time: $\left\langle \Delta r^2(t) \right\rangle = 10^{a+b\log(t)+c\{\log(t)\}^2}$ (3.4)

The logarithmic time derivative can also be computed

$$\frac{\partial \log\left(\Delta r^2(t) \right)}{\partial \log(t)} = b + 2c\log(t) \tag{3.5}$$

$G(s)$ can then be calculated from the method of relaxation spectra [41] explained in appendix A.

$$\tilde{G}(s) = \left. \frac{K_B T}{\pi a \left\langle \Delta r^2(t) \right\rangle \Gamma\left[1 + \left(\frac{\partial \log\left(\left\langle \Delta r^2(t) \right\rangle \right)}{\partial \log(t)} \right) \right]} \right|_{t=1/s} \tag{3.6}$$

To get $G(t)$, the time domain equivalent of $\tilde{G}(s)$, the inverse Laplace transform of $\tilde{G}(s)$ is taken using the canonical method of relaxation spectra [49]. $\tilde{G}(s)$ is then fit to $\sum_j G_j \frac{s}{s+\frac{1}{\tau_j}}$ using a nonlinear least squares routine. The τ_j values are chosen logarithmically to cover the desired range of s (usually from 10^{-1} to 10^{+4} seconds) and $G(t)$ is formed as a sum of decaying exponentials using weights G_j obtained from the least square fit. The frequency domain moduli G' and G'' are obtained as the unilateral Fourier cosine and sine transforms of $G(t)$. Briefly, by putting $s = i\omega$ in the functional form of $G(s)$ given by the weights G_j one obtains:

$$G'(\omega) = \sum_j \frac{G_j \omega^2 \tau_j^2}{1+\omega^2\tau_j^2} \text{ and } G''(\omega) = \sum_j \frac{G_j \omega\ \tau_j}{1+\omega^2\tau_j^2} \tag{3.7}$$

and $\left|G^*(\omega)\right|$ is obtained as the complex sum of G' and G'' given by

$$G = \left|G^*(\omega)\right| = \sqrt{\left(G'\right)^2 + \left(G''\right)^2} \tag{3.8}$$

$G, G'(\omega), G''(\omega)$ can all hence be calculated from MSD data, any of which provides insight into the mechanical properties of the medium. The higher the value of G the stiffer the medium. While the G values are functions of frequency, ω, the frequency 1 Hz [27, 41] is chosen in order to compare with values from literature.

Chapter Four: Results and Discussion

Neutrophils were aspirated gently into micropipettes with sizes ranging from 5 µm to 7.5 µm. The experiments were all carried out at room temperature and no attempt was made to change the temperature. During each aspiration the neutrophil was aspirated gently into the micropipette by applying just enough pressure to complete the aspiration. No further pressure was applied. All observations were made after a period of 3-5 minutes which was seen to be required for the cells to equilibrate to the new environment. The effect of mechanical deformation was quantified by using micropipettes of different sizes. The effect of biochemical mediators (adhesion molecules) was quantified by the coating the insides of the micropipettes with ICAM-1 in place of the control BSA. To elicit information on the effect of surface concentration of adhesion molecules on adhesion, the coatings were performed at two concentrations (0.1 µg/ml and 1 µg/ml). The results are accompanied by their discussion in the following sections.

4.1 Activation

In the first phase of trials, the relative effects of adhesion molecules and mechanical deformation on the activation of neutrophils was studied. A number of micropipette sizes were tried and with the sizes of cells were not uniform the deformation ratio ($R = D_c / D_p$) seemed a better parameter to represent the extent of mechanical deformation. Figure 4.1 shows the results of the study. It was seen that the percentage of cells that activated when aspirated into a micropipette was consistently smaller in control BSA coated micropipettes at any deformation ratio R than in ICAM-1 coated micropipettes. The results seemed to indicate that the presence of ICAM-1 had at least

some effect because its presence tends to make the cells more sensitive to activation. This result made a case for complete trials with adhesion molecules.

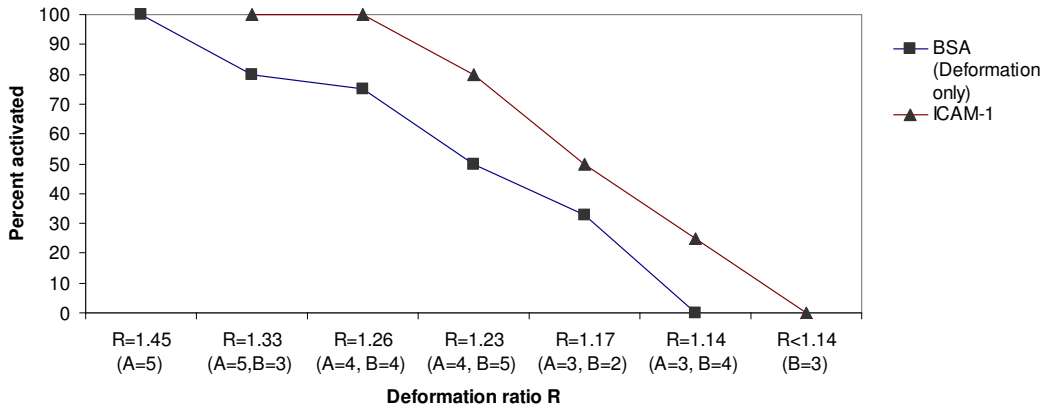

Figure 4.1. Results of micropipette aspirations to observe the relative effects of mechanical deformation and adhesion molecules on activation. The figure shows the percentage of cells that activated after aspiration at a deformation ratio R. A and B are the number of cells tried in BSA and ICAM-1 coated micropipettes respectively.

Inflammation in the body causes upregulation of the expression of adhesion molecules such as ICAM-1 on the endothelial cells lining the lung capillaries which is followed by sequestration of neutrophils from the blood stream. With activation being a step preceding extravasation, the result tied in well with in-vivo observations [1].

4.2 Deformation-only effect on micro-rheology

The results for the deformation only aspirations are shown in Fig. 4.2. The results show that there are regional rheological differences in a recently deformed neutrophil. With different number of data points in each region (unbalanced design) and multiple groups (regions >2) to be compared, a ‘Bonferroni’ correction had to be applied to the critical probabilities so as to keep the overall critical probability at 0.05. To this end, we

use the critical values from the t distribution, after applying a 'Dunn–Sidak' [50] correction for multiple comparisons. The analysis was performed using a multicomparison routine in MATLAB with a single factor ANOVA routine (anova1). The results of multiple comparisons are shown in Fig. 4.3. The body region is significantly stiffer ($p<0.05$) than the leading and trailing regions which are statistically indistinguishable in stiffness ($p<0.05$) from each other.

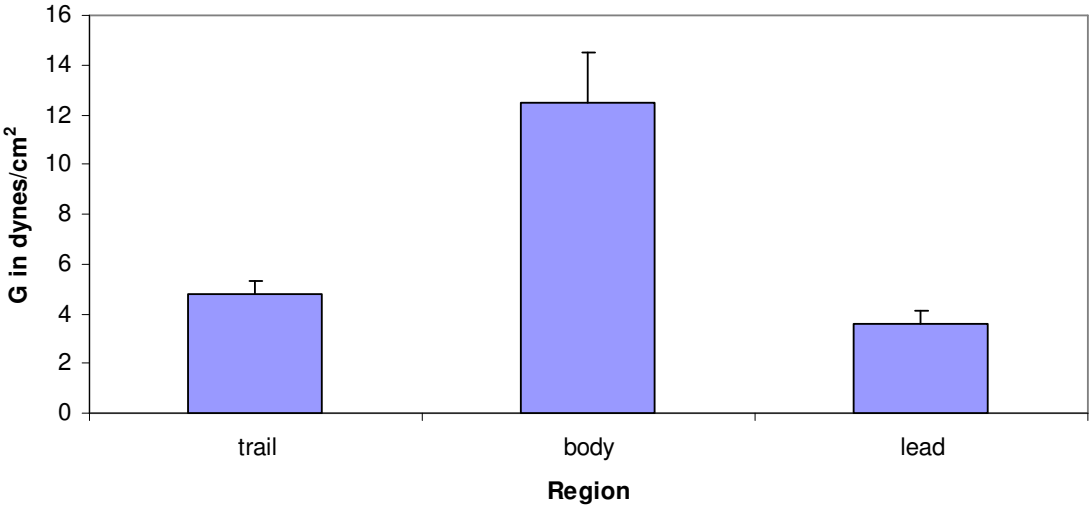

Figure 4.2. Modulus G (in dynes/cm^2) values in different cell regions for the deformation-only assay. The vertical bars are standard errors. The trailing and leading regions are both significantly ($P<0.05$ with Bonferroni correction) softer than the body region.

This contrasts with previous work by Yanai et al [27, 43, 44] where differences were seen between body and leading regions but the body and trailing regions were apparently indistinguishable. It should be noted however that these studies were not performed in circular chambers (representative of capillaries). The fact that the leading and trailing regions were indistinguishable in experiment agrees well with the experimental observation that once deformed and activated, the cell chooses the direction to move

independent of the direction it was aspirated in. The results indicate that at least some part of the neutrophil movement is achieved because the cell strains against the wall in the body region and uses this leverage to push out at the end caps. This agrees well with experiments showing more fluid like behavior at end caps and hence supports the idea that *flow into pseudopodia is pressure driven* [44].

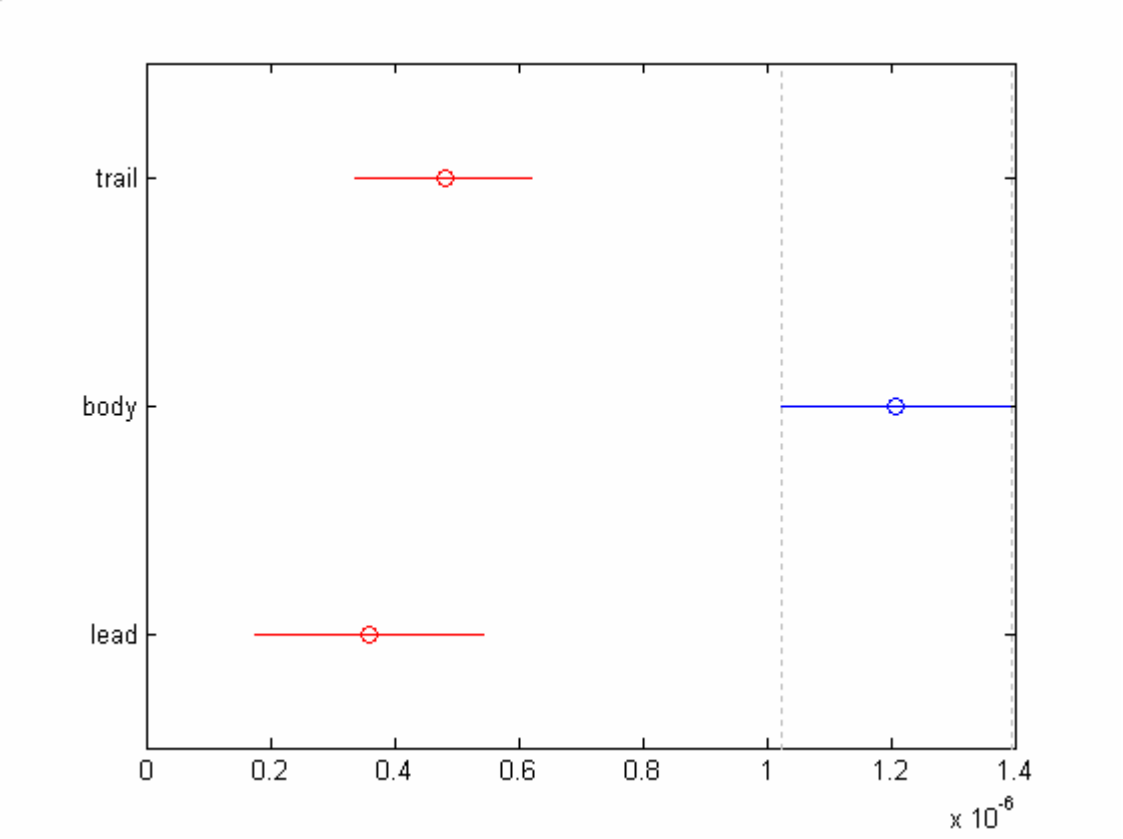

Figure 4.3. Statistical comparison diagram generated by MATLAB comparing viscoelastic moduli for the three regions in a cell to see the effects of deformation in the absence of adhesion molecules. The horizontal bars are 95% confidence intervals placed around the calculated marginal means in dynes/cm^2. The body region is significantly different from the endcaps.

Indeed, the few granules that were captured in the pseudopodia (data not shown) did seem to suggest a highly fluid medium. Cytoskeleton disruption was not exclusively

probed in the assay. Passive rounds cell have been reported to have G values ranging 100-700 dynes/cm^2 [27] while deformation reduced this G value to around 10 dynes/cm^2. The ten fold drop in viscoelastic moduli within seconds of aspiration, which was also seen in other recent work [27], can only be explained by the rapid depolymerization of actin and other constituents of the cytoskeleton. The results of this study agree with the theory that the cytoskeleton is largely responsible for the viscoelasticity of the passive cell.

4.3 Effect of adhesion molecules on micro-rheology

The effect of different surface concentrations of ICAM-1 on cell rheology was also investigated. For the concentrations tested (0.1 μg/ml and 1 μg/ml) no effect was found. While this can be taken to mean that only a critical ICAM-1 concentration is necessary to influence the neutrophils, there was some experimental uncertainty on how the two different ICAM-1 concentrations coat the inside surfaces of the micropipettes. It is possible that the coating procedure resulted in the saturation of the surface at both 0.1 and 1 μg/ml. With this uncertainty still unresolved, in other work in the lab, no attempt to analyze the effects of concentration on cell rheology was made and all data from ICAM-1 exposure was combined. The results for the inclusion of adhesion molecules are shown in Fig. 4.4.

Figure 4.4 shows that an increase in modulus was apparent in each of the three regions of the neutrophil. With different number of data points in each region (unbalanced design) and within BSA and ICAM-1 (Two factors: region and molecule) with multiple groups (regions >2) to be compared, a ‘Bonferroni’ correction had to be

applied to the critical probabilities so as to keep the overall critical probability at 0.05. To make the comparison, critical values from the t distribution after applying a 'Dunn–Sidak' [50] correction for multiple comparisons were used. The analysis was performed using a multicomparison routine in MATLAB with a *two factor ANOVA* routine (anovan) built to handle an unbalanced design. The results of the statistical analysis are shown and explained in Fig. 4.5 and Fig. 4.6. The results showed that adhesion molecules clearly increased the stiffness ($p<0.05$) of the cells while preserving the regional rheological differences seen with deformation-only BSA analysis.

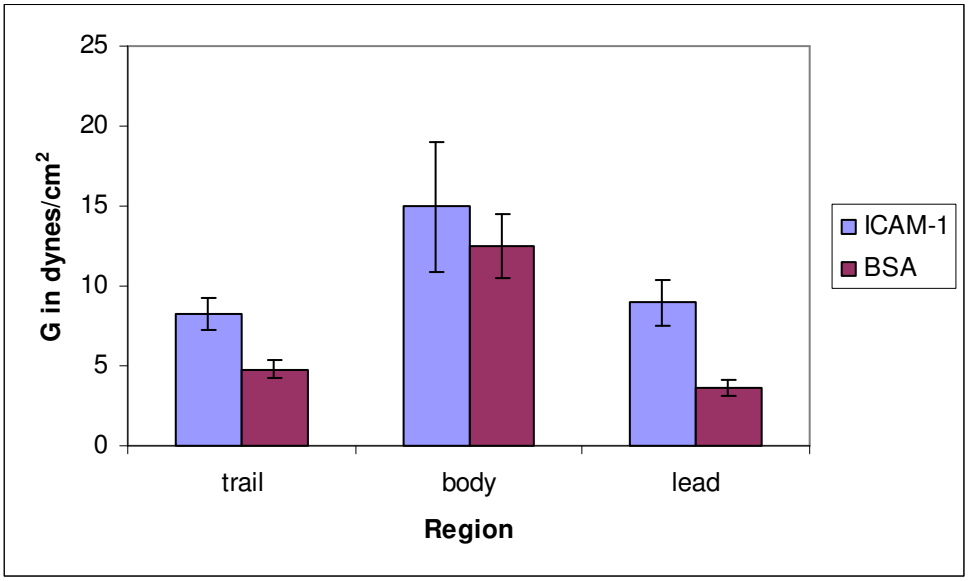

Figure 4.4. Comparison for modulus G (in dynes/cm^2) for BSA and ICAM-1. The vertical bars are standard errors. The trailing and leading regions appear softer than the body region in both cases. The results show a non-coincidental increase in stiffness with ICAM-1.

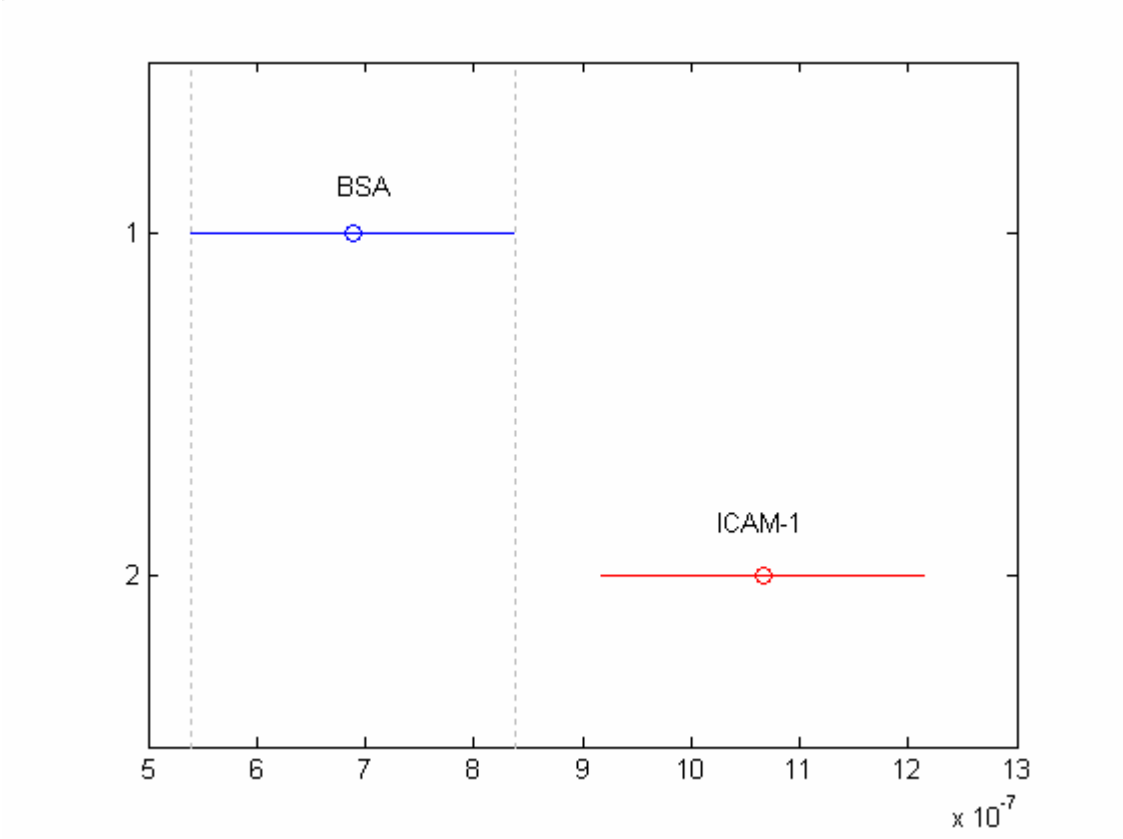

Figure 4.5. Statistical comparison diagram generated by MATLAB that compares the effects of BSA and ICAM-1 on stiffness. The horizontal bars are 95% confidence intervals placed around the calculated marginal means in dynes/cm^2. There is a significant increase in stiffness in the presence of ICAM-1.

The extensive studies [1, 3, 7, 51] that investigated the influence of adhesion molecules in capillaries all pointed to their redundancy in the margination phenomenon. These studies, however, also pointed to the fact that once sequestered, in inflamed lungs, adhesion molecules were required to keep the cells attached long enough to achieve extravasation. The attempts to identify the molecules that were required for sequestration argued against a major role for selectins [1] while in some studies ICAM-1 involved CD-11/CD18 binding pathways appeared to play a significant role [1, 52].

The contribution of adhesion molecules like ICAM-1 to prolonged neutrophil presence in inflamed lungs can be explained in terms of reduced deformability (increased

stiffness). The reduced deformability is necessary for the neutrophil to resist the flow pressure in preparation for increased area of contact and hence adhesion with the capillary surface (endothelial cell lined), all of which are prerequisites for successful extravasation of the neutrophil at the site of infection. This same increase in stiffness is seen in in-vitro studies presented here. The increase in stiffness has also been observed in-vivo [2], where it was shown that both neutrophils and endothelial cells stiffen up during adhesion, that is known to be mediated by adhesion molecules.

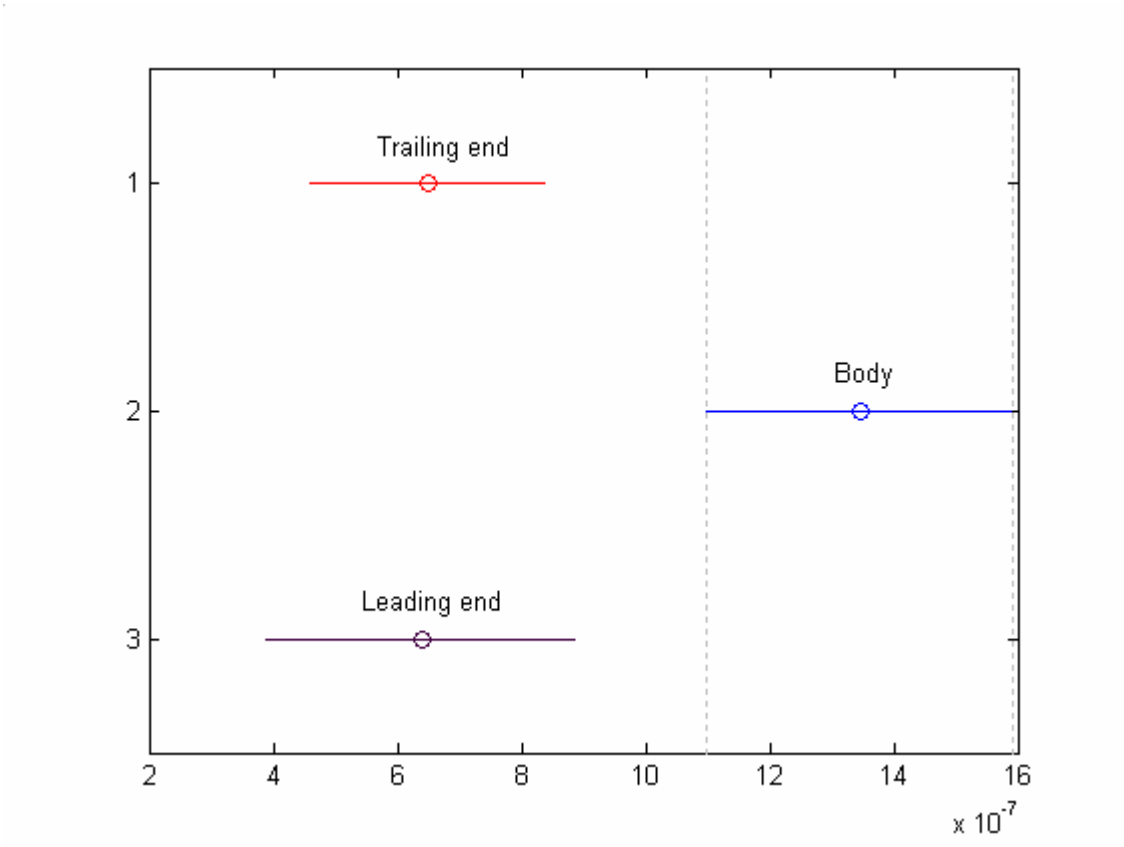

Figure 4.6. Results of a multiple comparison test (Dunn's test with Bonferroni correction) run on the regional viscoelasticity data obtained from ICAM-1 aspirations. The horizontal bars are 95% confidence intervals placed around the calculated marginal means. A significant regional difference in viscoelasticity is again seen in the presence of ICAM-1.

To sum up, the study theorizes the following steps in leukocyte adhesion in lung capillaries. The lung structure is responsible for the marginated pool of neutrophils in passive lungs caused by the requirement of the leukocytes to deform while passing through the narrow segments. In inflamed lungs the endothelial cells additionally express adhesion molecules such as ICAM-1 which cause an increased concentration (sequestration) of neutrophils in the capillaries. This is achieved by the stiffening of the neutrophils on exposure to the adhesion molecules. The increased stiffness improved ability to resist the force from blood flow in the capillary and to spend enough time adhered to the capillary to prepare for migration across the endothelial cell wall to the site of infection.

Chapter Five: Conclusions and Future Work

The objective of this study was to understand the effects of mechanical deformation and biochemical mediators (in the form of adhesion molecules such as ICAM-1) on the behavior of neutrophils in lung capillaries by observing their internal rheology. This was done using an in-vitro micropipette aspiration assay designed to mimic the physics of lung capillaries. Mechanical deformation was characterized by using a range of micropipette sizes coated with a control molecule (BSA) to prevent non-specific adhesion, simulating the absence of adhesion molecules. The presence of adhesion molecules was simulated by coating the micropipettes with ICAM-1, a molecule most commonly implicated in neutrophil sequestration in inflamed lungs.

The preliminary part of the study observed the extent of deformation achievable without activating the cells. This was initially quantified in terms of a critical deformation ratio. The ratio was found to be affected by the presence of adhesion molecules and the same information was used to select a range of capillary sizes that would probe the cells without activating them. While operating in this passive deformation range, the effects of mechanical deformation and the inclusion of adhesion molecules were studied by observing the internal viscoelastic moduli of the cells, which was a direct indicator of the cells stiffness.

The results indicated that neutrophils possess the ability to change their rheology extremely quickly in response to mechanical stimulus, a phenomenon explained by the polymerization and depolymerization of the cytoskeleton members. In addition the

neutrophils showed a regional rheological difference between the body region and the endcaps which has been partially observed in other studies [43, 44].

The next part of the study looked at the effects of adhesion molecules such as ICAM-1 on cell stiffness. It was seen that while the exposure to ICAM-1 preserved the regional rheological differences (Fig. 4.4 and Fig. 4.6), it caused an increase in the viscoelastic moduli indicating an increased stiffness (Fig. 4.4 and Fig. 4.5). This effect can be explained by the necessity of the neutrophil to 'stiffen-up' to resist the force from blood flow in the capillary in preparation for migration across the capillary tissue to the site of infection. Indeed, the same effect was seen experimentally when exposed endothelial cells treated with inflammatory mediator were exposed to neutrophils [2].

Further investigations on neutrophil adhesion using micropipettes as flow chambers should help answer many more questions on the leukocyte behavior in lung capillaries. Specifically, the assay may be used to better understand the roles played by the cytoskeleton in adhesion and the roles of each of the members of cytoskeleton network. This can be done using chemicals (such as cytochalasin D and nocodazole) which disrupt specific cytoskeleton members (actin and microtubules respectively). The assay may further be combined with staining agents for each of the cytoskeleton members to see the effects of mechanical deformation and adhesion molecules.

Chapter Six: Safety Measures

The regulations of Environment Health and Safety (EHS- Blood Borne Pathogens and Chemical Hygiene Program, Ohio University) were followed during research. The lab follows the EHS certified blood borne pathogen program and also has a certified blood spill cleaning protocol [47].

All procedures involving cells were done in the Bio-Safety Hood. The bio- waste is disposed in special biohazard disposal boxes picked up by 'Stericycle' whenever required [47]. All the lab members had an individual bio-safety kit and had taken the Hepatitis-B vaccine [47].

Chemicals were handled only in fume hoods and separate clearly marked storage spaces were used for storing flammable chemicals. Material Safety Data Sheets (MSDS) exist for all chemicals used in the lab and appropriate procedures were followed [47].

APPENDIX A

The connection between Brownian motion and local rheological properties was developed by Mason and Weitz [41, 42]. Consider a Brownian particle of mass *m* in a fluid with a generalized time dependent memory function $\zeta(t)$. Starting with the **Langevin** equation, we have

$$m\dot{v}(t) = f_r(t) - \int_0^t \zeta(t-t')v(t')dt' \tag{A1}$$

where v denotes velocity and $f_r(t)$ represents the random forces acting on the particle and includes the contribution from direct and stochastic sources. Assuming a Gaussian distribution for $f_r(t)$ with a mean zero and shall neglect this term for the following ensemble calculations.

Taking the Laplace transform of Eq. A1, and making use of the convolution theorem for Laplace transforms we get:

$$ms\,\tilde{v}(s) - m\,v(0) = -\tilde{\zeta}(s)\,\tilde{v}(s) \tag{A2}$$

Multiplying both sides by $v(0)$ and using the energy equipartition principle

$$m\langle v(0)v(0)\rangle = k_B T \tag{A3}$$

one obtains:

$$\left\langle \tilde{v}(0)\,\tilde{v}(s)\right\rangle = \frac{k_B T}{ms + \tilde{\zeta}(s)} \tag{A4}$$

We need to now relate the velocity correlation $\left\langle \tilde{v}(0)\,\tilde{v}(s)\right\rangle$ to the MSD $\left\langle \Delta\tilde{\bar{r}}^{\,2}(s)\right\rangle$.

For one dimensional motion from first principles we have:

$$x(t) = \int_o^t v(t')dt' \tag{A5}$$

Where we set $x(0) = 0$ at $t = 0$ for convenience so the mean squared x directed displacement is given by:

$$\left\langle x^2(t)\right\rangle = \left\langle \int_o^t v(t')dt' \int_o^t v(t'')dt'' \right\rangle = \int_o^t dt' \int_o^t dt'' \left\langle v(t')v(t'')\right\rangle \tag{A6}$$

where t' and t'' are just two variables for time. The last term in the angle brackets, $\left\langle v(t')v(t'')\right\rangle$ is the velocity correlation function [53]. This being a time-independent function, it may be written equivalently as $\left\langle v(0)v(\tau)\right\rangle$ where $\tau = t''-t'$, hence:

$$\left\langle x^2(t)\right\rangle = \int_o^t dt' \int_o^t d\tau \left\langle v(0)v(\tau)\right\rangle \tag{A7}$$

Noting that the correlation function is independent of time we can change the order of integration and the subsequent limits [53] to finally obtain :

$$\left\langle x^2(t)\right\rangle = \int_o^t d\tau \int_o^{t-\tau} dt' \left\langle v(0)v(\tau)\right\rangle + \int_{-t}^0 d\tau \int_{-\tau}^t dt' \left\langle v(0)v(\tau)\right\rangle \tag{A8}$$

that can be further simplified to:

$$\left\langle x^2(t)\right\rangle = \int_o^t d\tau \left\langle v(0)v(\tau)\right\rangle (t-\tau) + \int_{-t}^0 d\tau \left\langle v(0)v(\tau)\right\rangle (t+\tau) \tag{A9}$$

From the symmetry of correlation functions we have that $\left\langle v(0)v(\tau)\right\rangle = \left\langle v(0)v(-\tau)\right\rangle$ so Eq. A9 simplifies to:

$$\left\langle x^2(t)\right\rangle = 2\int_o^t d\tau (t-\tau)\left\langle v(0)v(\tau)\right\rangle \tag{A10}$$

A unilateral Laplace transform [54] of Eq. A10 using the convolution property gives us:

$$\left\langle \tilde{x}^{2}(s) \right\rangle = \frac{2\left\langle \tilde{v}(0)\tilde{v}(s) \right\rangle}{s^{2}} \tag{A11}$$

Equivalently for three dimensional motion we have:

$$\left\langle \Delta \tilde{r}^{2}(s) \right\rangle = \frac{6\left\langle \tilde{v}(0)\tilde{v}(s) \right\rangle}{s^{2}} \tag{A12}$$

From A12 and A4 we obtain:

$$\tilde{\zeta}(s) = \frac{6k_{B}T}{s^{2}\left\langle \Delta \tilde{r}^{2}(s) \right\rangle} - ms \tag{A13}$$

The contribution of the inertial term ms is only significant at very high frequencies and it can be neglected for now. Going back to the governing equation for viscoelastic deformations and expressing stress, τ versus strain history using Boltzmann's superposition, we have:

$$\tau(t) = \int_{0}^{t} dt' \eta(t-t')\dot{\gamma}(t') \tag{A14}$$

The viscoelastic moduli G' and G'', however, are stress versus strain functions and hence in the Laplace domain we would have:

$$\tilde{G}(s) = s\tilde{\eta}(s) \tag{A15}$$

To complete the analysis, however, we need a relation between the bulk frequency-dependent viscosity $\eta(\omega)$ and the memory function ζ in the Langevin equation. For this we make the assumption that the Stokes law would remain valid for the particle.

Hence we have:

$$\tilde{\eta}(s) = \frac{\tilde{\zeta}(s)}{6\pi a} \tag{A16}$$

where *a* is the particle radius. Plugging Eq. A13 into Eq. A15, we have:

$$\tilde{G}(s) = s\tilde{\eta}(s) = s \times \frac{6k_B T}{s^2 \left\langle \Delta \tilde{r}^2(s) \right\rangle} \times \frac{1}{6\pi a} = \frac{k_B T}{\pi a s \left\langle \Delta \tilde{r}^2(s) \right\rangle} \tag{A17}$$

This equations is the frequency dependent generalized form of the Stokes-Einstein equation (Eq. 1.3 in text) abbreviated as GSER.

Eq. A17 in Fourier domain would appear as follows:

$$G^*(\omega) = \frac{k_B T}{\pi a i\omega F_U \left\langle \Delta \bar{r}^2(t) \right\rangle} \tag{A18}$$

where F_U is the unilateral Fourier transform for $s = i\omega$

Eq. A17 however requires the MSD, $\Delta \bar{r}^2$ in Laplace domain, which would have to calculated numerically and would hence introduce error. Mason et al. [41, 42] introduce instead a numerical approximation to the Laplace transform by using a power law expansion around a particular frequency ω given by:

$$\left\langle \Delta \bar{r}^2(t) \right\rangle = \left\langle \Delta \bar{r}^2(1/\omega) \right\rangle \times (\omega t)^{\alpha(\omega)} \tag{A19}$$

$$and \ \alpha(\omega) = \left(\frac{\partial \log\left(\left\langle \Delta r^2(t) \right\rangle \right)}{\partial \log(t)} \right)_{t=1/\omega} \tag{A20}$$

The Fourier transform F_U of Eq. A19 is evaluated and a series of approximations carried out to give:

$$\left|G^*(\omega)\right| = \frac{k_B T}{\pi a \left\langle \Delta r^2 (1/\omega) \right\rangle \Gamma\left[1+\alpha(\omega)\right]} \tag{A21}$$

which then translates to:

$$\tilde{G}(s) = \left. \frac{k_B T}{\pi a \left\langle \Delta r^2 (t) \right\rangle \Gamma\left[1+\left(\frac{\partial \log\left(\left\langle \Delta r^2 (t) \right\rangle\right)}{\partial \log(t)}\right)\right]} \right|_{t=1/s} \tag{A22}$$

This is Eq. 3.6 in the main text.

Glossary of Terms

ANOVA	Analysis of variance
BSA	Bovine serum albumin
DIC	Differential interference contrast
DPBS-	Dulbecco's phosphate buffered saline without calcium/magnesium
DPBS+	Dulbecco's phosphate buffered saline with calcium/magnesium
ECM	Extracellular matrix
fMLP	formyl-methionyl-leucyl-phenylalanine
GSER	Generalized Stokes Einstein relation
HBSS-	Hanks balanced salt solution without calcium
HBSS+	Hanks balanced salt solution with calcium
ICAM	Intercellular adhesion molecule
ID	Inner diameter
Ig	Immunoglobulin (family)
LAD	Leukocyte adhesion deficiency
LPS	Lipopolysaccharide
Margination	Increased concentration of leukocytes in non-inflamed lungs.
MSD	Mean square displacement
MSDS	Material safety data sheets
RBC	Red blood cell
Sequestration	Increased leukocyte concentration in lungs following inflammation.
VCAM	Vascular cellular adhesion molecule
WBC	White blood cell
NA	Numerical aperture

References

1. Doerschuk, C.M., Mechanisms of leukocyte sequestration in inflamed lungs. *Microcirculation*, **8**:71-88, 2001.

2. Wang, Q. and C.M. Doerschuk, Neutrophil-Induced Changes in the Biomechanical Properties of Endothelial Cells: Roles of ICAM-1 and Reactive Oxygen Species. *J Immunol*, **164**:6487-6494, 2000.

3. Gebb, S.A., J.A. Graham, C.C. Hanger, P.S. Godbey, R.L. Capen, C.M. Doerschuk, and W.W. Wagner Jr, Sites of leukocyte sequestration in the pulmonary microcirculation. *Journal of Applied Physiology*, **79**:493-497, 1995.

4. Doerschuk, C.M., W. Quinlan, N. Doyle, D. Bullard, D. Vestweber, M. Jones, F. Takei, P. Ward, and A. Beaudet, The role of P-selectin and ICAM-1 in acute lung injury as determined using blocking antibodies and mutant mice. *J Immunol*, **157**:4609-4614, 1996.

5. Kuebler, W.M., J. Borges, A. Sckell, G.E.H. Kuhnle, K. Bergh, K. Messmer, and A.E. Goetz, Role of L-Selectin in Leukocyte Sequestration in Lung Capillaries in a Rabbit Model of Endotoxemia. *Am J Respir Crit Care Med*, **161**:36-43, 2000.

6. Doerschuk, C.M., Leukocyte trafficking in alveoli and airway passages. *Respiratory Research*, **1**:136-140, 2000.

7. Doerschuk, C.M., R.K. Winn, H.O. Coxson, and J.M. Harlan, CD18-Dependent and -independent mechanisms of neutrophil emigration in the pulmonary and systemic microcirculation of rabbits. *Journal of Immunology*, **144**:2327-2333, 1990.

8. Bruce Alberts, Dennis Bray, Julian Lewis, Martin Raff, Keith Roberts, James D. Watson, *Molecular Biology of the Cell*. 2002: Garland Publications. 1463 pp.

9. Ley, K., *Physiology of Inflammation*. 2001: Oxford University Press, New York. 546 pp.

10. Springer, T.A., Traffic signals for lymphocyte recirculation and leukocyte emigration: the multistep paradigm. *Cell*, **76**:301-14, 1994.

11. Andonegui, G., C.S. Bonder, F. Green, S.C. Mullaly, L. Zbytnuik, E. Raharjo, and P. Kubes, Endothelium-derived toll-like receptor-4 is the key molecule in LPS-induced neutrophil sequestration into lungs. *Journal of Clinical Investigation*, **111**:1011-1020, 2003.

12. Bals, R., Lipopolysaccharide and the lung: a story of love and hate. *Eur Respir J*, **25**:776-777, 2005.

13. Stoolman, L.M., T.A. Yednock, and S.D. Rosen, Homing receptors on human and rodent lymphocytes--evidence for a conserved carbohydrate-binding specificity. *Blood*, **70**:1842-50, 1987.

14. Hahne, M., U. Jager, S. Isenmann, R. Hallmann, and D. Vestweber, Five tumor necrosis factor-inducible cell adhesion mechanisms on the surface of mouse endothelioma cells mediate the binding of leukocytes. *J Cell Biol*, **121**:655-64, 1993.

15. Lafrenie, R.M., M.R. Buchanan, and F.W. Orr, Adhesion molecules and their role in cancer metastasis. *Cell Biophys*, **23**:3-89, 1993.

16. Cheresh, D.A., Integrins in thrombosis, wound healing and cancer. *Biochem Soc Trans*, **19**:835-8, 1991.

17. Herlyn, M. and S.B. Malkowicz, Regulatory pathways in tumor growth and invasion. *Lab Invest*, **65**:262-71, 1991.

18. Hynes, R.O., Integrins: a family of cell surface receptors. *Cell*, **48**:549-54, 1987.

19. Ruoslahti, E., Integrins. *J Clin Invest*, **87**:1-5, 1991.

20. Hynes, R.O., Integrins: versatility, modulation, and signaling in cell adhesion. *Cell*, **69**:11-25, 1992.

21. Ruoslahti, E. and M.D. Pierschbacher, Arg-Gly-Asp: a versatile cell recognition signal. *Cell*, **44**:517-8, 1986.

22. Kirchhofer, D., J. Grzesiak, and M.D. Pierschbacher, Calcium as a potential physiological regulator of integrin-mediated cell adhesion. *J Biol Chem*, **266**:4471-7, 1991.

23. Argraves, W.S., S. Suzuki, H. Arai, K. Thompson, M.D. Pierschbacher, and E. Ruoslahti, Amino acid sequence of the human fibronectin receptor. *J Cell Biol*, **105**:1183-90, 1987.

24. Law, S.K., J. Gagnon, J.E. Hildreth, C.E. Wells, A.C. Willis, and A.J. Wong, The primary structure of the beta-subunit of the cell surface adhesion glycoproteins LFA-1, CR3 and p150,95 and its relationship to the fibronectin receptor. *Embo J*, **6**:915-9, 1987.

25. Hemler, M.E., VLA proteins in the integrin family: structures, functions, and their role on leukocytes. *Annu Rev Immunol*, **8**:365-400, 1990.

26. Borregaard, N. and J.B. Cowland, Granules of the Human Neutrophilic Polymorphonuclear Leukocyte. *Blood*, **89**:3503-3521, 1997.

27. Yap, B. and R.D. Kamm, Mechanical deformation of neutrophils into narrow channels induces pseudopod projection and changes in biomechanical properties. *J Appl Physiol*, **98**:1930-1939, 2005.

28. Burns, A.R., C.W. Smith, and D.C. Walker, Unique structural features that influence neutrophil emigration into the lung. *Physiological Reviews*, **83**:309-336, 2003.

29. Tees, D.F.J., P. Sundd, and D.J. Goetz, A Flow Chamber for Capillary Networks: Leukocyte Adhesion in Capillary-Sized, Ligand-Coated Micropipettes, in *Principles of Cellular Engineering*, M. King, Editor. Elsevier: New York. 213-232, 2005

30. Lau, D., H. Mollnau, J.P. Eiserich, B.A. Freeman, A. Daiber, U.M. Gehling, J. Brummer, V. Rudolph, T. Munzel, T. Heitzer, T. Meinertz, and S. Baldus, Myeloperoxidase mediates neutrophil activation by association with CD11b/CD18 integrins. *Proc Natl Acad Sci USA*, **102**:431-436, 2005.

31. Guntheroth, W.G., D.L. Luchtel, and I. Kawabori, Pulmonary microcirculation: tubules rather than sheet and post. *J Appl Physiol*, **53**:510-515, 1982.

32. Picker, L.J., R.A. Warnock, A.R. Burns, C.M. Doerschuk, E.L. Berg, and E.C. Butcher, The neutrophil selectin LECAM-1 presents carbohydrate ligands to the vascular selectins ELAM-1 and GMP-140. *Cell*, **66**:921-33, 1991.

33. Evans, E. and B. Kukan, Passive material behavior of granulocytes based on large deformation and recovery after deformation tests. *Blood*, **64**:1028-35, 1984.

34. Yeung, A. and E. Evans, Cortical shell-liquid core model for passive flow of liquid-like spherical cells into micropipets. *Biophys J*, **56**:139-149, 1989.

35. Evans, E. and D. Needham, Physical properties of surfactant bilayer membranes: thermal transitions, elasticity, rigidity, cohesion and colloidal interactions. *J Phys Chem*, **91**:4219 - 4228, 1987.

36. Hochmuth, R.M., Micropipette aspiration of living cells. *J Biomech*, **33**:15-22, 2000.

37. Tran-Son-Tay, R., D. Needham, A. Yeung, and R.M. Hochmuth, Time-dependent recovery of passive neutrophils after large deformation. *Biophys J*, **60**:856-66, 1991.

38. Bathe, M., A. Shirai, C.M. Doerschuk, and R.D. Kamm, Neutrophil Transit Times through Pulmonary Capillaries: The Effects of Capillary Geometry and fMLP-Stimulation. *Biophys J*, **83**:1917-1933, 2002.

39. Tran-Son-Tay R, K.T.r., Zhelev DV, Hochmuth RM, Numerical simulation of the flow of highly viscous drops down a tapered tube. *J Biomech Eng*, **116**:172-177, 1994.

40. Drury, J.L. and M. Dembo, Hydrodynamics of micropipette aspiration. *Biophys J*, **76**:110-28, 1999.

41. Mason, T.G., K. Ganesan, J.H. van Zanten, D. Wirtz, and S.C. Kuo, Particle Tracking Microrheology of Complex Fluids. *Phys Rev Lett*, **79**:3282-3285, 1997.

42. Mason, T.G. and D.A. Weitz, Optical measurements of frequency-dependent linear viscoelastic moduli of complex fluids. *Phys Rev Lett*, **74**:1250-1253, 1995.

43. Yanai, M., J.P. Butler, T. Suzuki, A. Kanda, M. Kurachi, H. Tashiro, and H. Sasaki, Intracellular elasticity and viscosity in the body, leading, and trailing regions of locomoting neutrophils. *Am J Physiol Cell Physiol*, **277**:C432-440, 1999.

44. Yanai, M., J.P. Butler, T. Suzuki, H. Sasaki, and H. Higuchi, Regional rheological differences in locomoting neutrophils. *Am J Physiol Cell Physiol*, **287**:C603-611, 2004.

45. Sundd, P., Tees lab data.

46. Tees, D.F.J., R.E. Waugh, and D.A. Hammer, A Microcantilever Device to Assess the Effect of Force on the Lifetime of Selectin-Carbohydrate Bonds. *Biophys J*, **80**:668-682, 2001.

47. Tees, D.F.J., *lab protocols*.

48. Shinya Inoué, K.R.S., *Video Microscopy : The Fundamentals*. Second ed. 1997: Plenum Press. 741 pp.

49. R. B. Bird, R.C. Armstrong., and O. Hassager, *Dynamics of Polymeric Liquids*. 1977, New York: John Wiley and Sons. 773 pp.

50. Wilcox, R.R., *New Statistical Procedures for the Social Sciences: Modern Solutions to Basic Problems*. 1987: Lawrence Erlbaum Assoc Inc 423 pp.

51. Carlos, T.M. and J.M. Harlan, Leukocyte-endothelial adhesion molecules. *Blood*, **84**:2068-101, 1994.

52. Kubo, H., N.A. Doyle, L. Graham, S.D. Bhagwan, W.M. Quinlan, and C.M. Doerschuk, L- and P-Selectin and CD11/CD18 in Intracapillary Neutrophil Sequestration in Rabbit Lungs. *Am J Respir Crit Care Med*, **159**:267-274, 1999.

53. Reif, F., *Fundamentals of statistical and thermal physics*. 1965, New York: McGraw-Hill. 651 pp.

54. Oppenheim, A.V., A.S. Willsky, and I.T. Young, *Signals and systems*. 1983, Englewood Cliffs, N.J: Prentice-Hall. 796 pp.